Born-Padé method for scattering by a diffraction grating
s polarization

van der Sijs, Thomas A.; El Gawhary, Omar; Urbach, H. Paul

DOI
10.1117/12.3015272

Publication date
2024

Document Version
Final published version

Published in
Nanophotonics X

Born-Padé method for scattering by a diffraction grating: s polarization

Thomas A. van der Sijs[a], Omar El Gawhary[a], and H. Paul Urbach[a]

[a]Optics Research Group, Imaging Physics Department, Delft University of Technology, Van der Waalsweg 8, 2628 CH Delft, The Netherlands

ABSTRACT

We use a rigorous vector Born series to solve electromagnetic scattering by a diffraction grating. To deal with possible divergence of the Born series, we compute Padé approximants of the Born series to retrieve the solution regardless. Besides results of the Born-Padé method for an example grating, for which the Born series diverges, we show analytical expressions for a two-layer grating in the case of s polarization. This gives insight into the convergence behavior of the Born series as function of the angle of incidence, for instance.

Keywords: Born series, scattering, electromagnetism, diffraction grating, Padé approximants

1. INTRODUCTION

The analysis of periodic structures, such as diffraction gratings, is of interest for many practical applications, ranging from optical metrology techniques to photovoltaics.[1,2] Often, numerical methods such as rigorous coupled-wave analysis are used,[3] where large linear systems are inversed. These methods tend to be 'black-box' methods, as the solution is yielded at once or with numerical optimization strategies that do not give insight in the physical mechanisms that generate the scattered field. However, a more analytical method that better reflects the underlying physical mechanisms is the Born series, building the scattered field solution step by step, each step corresponding to a certain scattering event.

In our recent work,[4] we presented a vectorial Born series and its semi-analytical implementation for a diffraction grating. As is known for the Born series, it converges only in a limited number of cases, which limits its usefulness. We employed Padé approximation to extract a solution for the electric field from the Born series, even if it diverges. The results can be calculated on a computer for any kind of one-dimensional (1D) grating, but analytical results may also be obtained. Here, we show the vectorial Born series for a grating and show the scalar equations for the case of s polarization (under classical incidence). We derive analytical expressions for the Born approximation for this case, from which we can obtain an indication of the convergence behavior of the Born series as function of parameters such as the pitch or permittivity.

2. VECTOR BORN SERIES AND PADÉ APPROXIMATION

We follow the method developed in our recent work.[4] We consider time-harmonic fields with time dependence $\mathrm{e}^{-\mathrm{i}\omega t}$, where $\omega > 0$ is the angular frequency. The scatterer has some (possibly complex) relative permittivity $\varepsilon_r(\mathbf{r})$ with positive imaginary part, while magnetization is neglected. We develop a Born series for the vector Helmholtz equation $\nabla \times \nabla \times \mathbf{E}(\mathbf{r}) - k_0^2 \varepsilon_r(\mathbf{r}) = 0$, with $k_0 = 2\pi/\lambda$ the wavenumber in vacuum. The problem becomes a perturbation problem when a perturbation parameter σ is introduced:

$$\nabla \times \nabla \times \mathbf{E}(\mathbf{r}) - k_0^2(1 + \sigma \Delta\varepsilon_r(\mathbf{r})) = 0, \tag{1}$$

with $\Delta\varepsilon_r(\mathbf{r}) = \varepsilon_r(\mathbf{r}) - 1$ the permittivity contrast relative to the background ($\varepsilon_r = 1$). Both the vector potential $\mathbf{A}(\mathbf{r})$ and electric field $\mathbf{E}(\mathbf{r})$ are expanded as a power series in σ:

$$\mathbf{E}(\mathbf{r}) = \sum_{\ell=0}^{\infty} \mathbf{E}_\ell(\mathbf{r})\sigma^\ell \quad \text{and} \quad \mathbf{A}(\mathbf{r}) = \sum_{\ell=0}^{\infty} \mathbf{A}_\ell(\mathbf{r})\sigma^\ell. \tag{2}$$

Further author information: (Send correspondence to T.A.S.)
T.A.S.: E-mail: t.a.vandersijs@tudelft.nl

Nanophotonics X, edited by David L. Andrews, Angus J. Bain, Antonio Ambrosio, Proc. of SPIE Vol. 12991, 129910V · © 2024 SPIE
0277-786X · doi: 10.1117/12.3015272

Starting from some incident electric field $\mathbf{E}^{(i)}(\mathbf{r})$, the higher-order terms of these Born series can be computed recurrently:

$$\mathbf{A}_{\ell+1}(\mathbf{r}) = -\mathrm{i}\omega\varepsilon_0 \int_{\mathbf{r}'} G_0(\mathbf{r};\mathbf{r}')\Delta\varepsilon_r(\mathbf{r}')\mathbf{E}_\ell(\mathbf{r}')\,\mathrm{d}^3r', \tag{3}$$

$$\mathbf{E}_{\ell+1}(\mathbf{r}) = \mathrm{i}\omega\mu_0\mathbf{A}_{\ell+1}(\mathbf{r}) - \frac{1}{\mathrm{i}\omega\varepsilon_0}\nabla\left(\nabla\cdot\mathbf{A}_{\ell+1}(\mathbf{r})\right), \tag{4}$$

where $G_0(\mathbf{r};\mathbf{r}') = \mathrm{e}^{\mathrm{i}k_0|\mathbf{r}-\mathbf{r}'|}/4\pi|\mathbf{r}-\mathbf{r}'|$ is the scalar 3D free-space Green's function. The recurrence is a two-step process, where first $\mathbf{A}_{\ell+1}$ is computed component-wise from $\mathbf{E}_\ell$. Then, $\mathbf{A}_{\ell+1}$ is used to compute the next electric field order $\mathbf{E}_{\ell+1}$, and it is in this step that depolarization effects can take place when taking the gradient of the divergence of $\mathbf{A}_{\ell+1}$.

2.1 Padé approximation

The second step of the presented method is the computation of Padé approximants from the terms in the Born series. As the Born series converges only for a limited number of cases, this allows us to use the Born series to retrieve a solution even in cases where the series diverges. The region of convergence is determined by the spectrum of the Lippmann-Schwinger integral operator.[5,6] To retrieve a solution for $\mathbf{E}$ outside the region of convergence, the Padé representation is equated to the Born representation within the region of convergence. The Padé approximants can then also be used outside the Born series' region of convergence. We consider symmetric Padé approximants,[7] rational functions for which the order of the polynomial in the numerator and denominator are the same:

$$P_N^N(\mathbf{r},\sigma) = \frac{\sum_{m=0}^{N} A_m(\mathbf{r})\sigma^m}{1+\sum_{n=1}^{N} B_n(\mathbf{r})\sigma^n}. \tag{5}$$

Hence, there are in total $2N+1$ unknown Padé coefficients A_m and B_n that have to be computed from the Born series. This entails solving a relatively small linear system of $2N+1$ equations for every point $\mathbf{r}$ on a discretized grid. In the end, the perturbation parameter σ is set to 1 to obtain the Padé approximant for our problem.

3. APPLICATION TO A DIFFRACTION GRATING

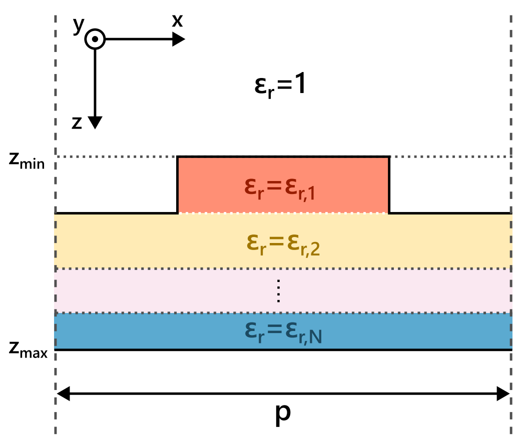

Figure 1. One period of an example of a 1D diffraction grating with the definition of the coordinate system (x, y, z). The positive y direction points out of the paper. For the case of s polarization, the electric field is perpendicular to the paper, along the grating grooves.

We consider a 1D periodic scatterer that is p-periodic in x, invariant in y, and bounded in z (between $z_{\min} < z < z_{\max}$). See Fig. 1 for a schematic depiction of the problem. Due to the periodicity of the grating problem, the permittivity distribution can be decomposed into a Fourier series:

$$\Delta\varepsilon_r(x,z) = \sum_{m=-\infty}^{\infty} \Delta\varepsilon_r^{(m)}(z)\mathrm{e}^{\mathrm{i}2\pi xm/p}. \tag{6}$$

Furthermore, the electric field $\mathbf{E}$ and its Born series will be pseudo-periodic, i.e.,

$$\mathbf{E}_\ell(\mathbf{r}) = \sum_{m=-\infty}^{\infty} \mathbf{E}_\ell^{(m)}(z)\, \mathrm{e}^{\mathrm{i}2\pi\left(q_x^{(i)}+m/p\right)x+\mathrm{i}2\pi q_y^{(i)} y}, \tag{7}$$

with $\mathbf{E}_\ell^{(m)}(z)$ the Fourier coefficients of the ℓth Born term, and $q_x^{(i)} = k_x^{(i)}/2\pi$ and $q_y^{(i)} = k_y^{(i)}/2\pi$ the spatial frequencies of the incident plane wave (having amplitude 1)

$$\mathbf{E}^{(i)}(x,z) = \mathrm{e}^{\mathrm{i}2\pi(q_x^{(i)}x+q_y^{(i)}y+q_z^{(i)}z)}\hat{\mathbf{e}}_0, \tag{8}$$

with $\hat{\mathbf{e}}_0$ the polarization unit vector.

3.1 Method for s polarization

From now on, we will only consider s polarization under classical incidence ($q_y^{(i)} = 0$), for which only the E_y component is nonzero, which we denote by U. The two-step recurrence (Eqs. (3) and (4)) reduces to the recurrence relation for the scalar Born series,[8] i.e., the scalar Lippmann-Schwinger operator:

$$U_{\ell+1}(\mathbf{r}) = k_0^2 \int_{\mathbf{r}'} G_0(\mathbf{r};\mathbf{r}')\Delta\varepsilon_r(\mathbf{r}')U_\ell(\mathbf{r}')\,\mathrm{d}^3r'. \tag{9}$$

The implementation of this recurrence relation for the 1D grating problem can be retrieved from our vectorial result.[4] We refer to Appendix A for the general vectorial equation that works for any incidence (classical and conical) and any polarization. The recurrence starts with the incident field

$$U^{(i)}(x,z) = \mathrm{e}^{\mathrm{i}2\pi(q_x^{(i)}x+q_z^{(i)}z)}, \tag{10}$$

with $q_z^{(i)} = \sqrt{q_0^2 - q_x^{(i)}}$ and $q_0 = k_0/2\pi$. For computation of the $(\ell+1)$st Born order, the Fourier coefficients of the induced current density due to the ℓth order field are used as input:

$$\Delta\varepsilon_r(x,z)U_\ell(x,z) = \sum_{m=-\infty}^{\infty} c_\ell^{(m)}(z)\mathrm{e}^{\mathrm{i}2\pi q_{xm}x}, \tag{11}$$

with $q_{xm} = q_x^{(i)} + m/p$ the x-component of the wave vector of the mth diffraction order. The recurrence relation consists of the computation of two 1D integrals for every Fourier mode m:

$$U_{\ell+1}^{(m)}(z) = \mathrm{i}\pi\frac{q_0^2}{q_{zm}}\left[C_{\ell,<}^{(m)}(z) + C_{\ell,>}^{(m)}(z)\right], \tag{12}$$

with $C_{\ell,<}^{(m)}(z)$ and $C_{\ell,>}^{(m)}(z)$ integrals over z:

$$C_{\ell,<}^{(m)}(z) = \begin{cases} \int_{z_{\min}}^{z} c_\ell^{(m)}(z')\mathrm{e}^{\mathrm{i}2\pi q_{zm}(z-z')}\,\mathrm{d}z' & \text{if } z_{\min} < z, \\ 0 & \text{if } z_{\min} > z, \end{cases} \tag{13}$$

$$C_{\ell,>}^{(m)}(z) = \begin{cases} \int_{z}^{z_{\max}} c_\ell^{(m)}(z')\mathrm{e}^{\mathrm{i}2\pi q_{zm}(z'-z)}\,\mathrm{d}z' & \text{if } z_{\max} > z, \\ 0 & \text{if } z_{\max} < z, \end{cases} \tag{14}$$

and with q_{zm} defined as

$$q_{zm} = \begin{cases} \sqrt{q_0^2 - q_{xm}^2}, & q_{xm}^2 \le q_0^2, \\ \mathrm{i}\sqrt{q_{xm}^2 - q_0^2}, & q_{xm}^2 > q_0^2. \end{cases} \tag{15}$$

Note that we are essentially solving a scalar 1D scattering problem for every order m; the two integrals are due to the absolute value in $\mathrm{e}^{\mathrm{i}2\pi q_z|z-z'|}$ in the plane wave expansion of the Green's function. At the end of a iteration, we obtain the real space field $U_{\ell+1}(x,z)$ by summing the computed Fourier modes. This then serves as the input to the next iteration.

3.2 Analytical first Born order for a simple grating

To get a better insight into how the scattered field is built up using the Born series, we derive analytical expressions for the first Born order for a simple system. We consider a two-layer grating: a rectangular grating layer on top of a planar layer (a slab). The grating layer is located in the domain $z_1 < z \leq z_2$ and the slab layer in $z_2 < z \leq z_3$. Both layers are of the same material with some (possibly complex) permittivity contrast $\Delta\varepsilon_r$. The grating layer has a rectangular profile with pitch p and linewidth a and is symmetric around $x = 0$. It can be derived that its periodic permittivity distribution (see Eq. (6)) has Fourier coefficients

$$\Delta\varepsilon_r^{(m)}(z) = \Delta\varepsilon_r \frac{a}{p} \mathrm{sinc}\left(\frac{\pi m a}{p}\right), \quad z_1 < z \leq z_2. \tag{16}$$

When we are to compute the scattered first Born order, the field inside the grating layer will contain a contribution from the slab and a self-contribution from the grating layer itself. For the scattered first order inside the slab, it is the other way around. The first-order field at any point is thus the field scattered by the slab plus the field scattered by the grating, respectively:

$$U_1(x,z) = U_{1,s}(x,z) + U_{1,g}(x,z). \tag{17}$$

It is possible to consider the contributions from different parts of the structure separately, because the Born recurrence relation (Eq. (9)) is linear in $\Delta\varepsilon_r$. The contribution from each layer is different depending on whether it concerns the field inside the layer itself, or the field outside it. The integrals in Eqs. (13) and (14) are namely only both nonzero inside the considered layer, while one of the two evaluates to 0 outside it. Here, we only show the results for s polarization, although the expressions for the rigorous vectorial case can also be found.

3.2.1 Field scattered by slab

Since the permittivity of the slab is homogeneous, its Fourier decomposition only has an $m = 0$ component. The field scattered by the slab will thus not contain any diffraction orders other than the $m = 0$ order. The field scattered by the slab reads, inside the grating layer and inside the slab, respectively:

$$U_{1,s}(x,z) = \mathrm{i}\pi \frac{q_0^2}{q_z^{(i)}} \Delta\varepsilon_r \mathrm{e}^{\mathrm{i}2\pi(q_x^{(i)}x - q_z^{(i)}z)} \frac{1}{\mathrm{i}4\pi q_z^{(i)}} \left[\mathrm{e}^{\mathrm{i}4\pi q_z^{(i)} z_3} - \mathrm{e}^{\mathrm{i}4\pi q_z^{(i)} z_2}\right], \qquad z_1 < z < z_2, \tag{18}$$

$$U_{1,s}(x,z) = \mathrm{i}\pi \frac{q_0^2}{q_z^{(i)}} \Delta\varepsilon_r \mathrm{e}^{\mathrm{i}2\pi q_x^{(i)}x} \left[\mathrm{e}^{\mathrm{i}2\pi q_z^{(i)}z}(z - z_2) + \frac{1}{\mathrm{i}4\pi q_z^{(i)}} \mathrm{e}^{-\mathrm{i}2\pi q_z^{(i)}z}\left(\mathrm{e}^{\mathrm{i}4\pi q_z^{(i)}z_3} - \mathrm{e}^{\mathrm{i}4\pi q_z^{(i)}z}\right)\right], \quad z_2 < z < z_3. \tag{19}$$

Inside the grating layer, the field is a plane wave with the same q_x and q_z as the incident field, only propagating upwards ($-z$ direction) from the grating, since it originates from the slab (located at larger z). Also, we see that the self-contribution of the slab consists of an upward and a downward propagating wave, which are modulated by an amplitude that depends on the location z inside the grating layer. Moreover, note that the expressions agree at the interface $z = z_2$.

3.2.2 Field scattered by grating

As the permittivity contrast $\Delta\varepsilon_r$ of the grating layer has nonzero Fourier components for every m, the field scattered by the grating layer will be a sum over diffraction orders. The self-contribution of the grating is

$$\begin{aligned} U_{1,g}(x,z) = \sum_{m=-\infty}^{\infty} \mathrm{i}\pi \frac{q_0^2}{q_{zm}} \Delta\varepsilon_r^{(m)} \mathrm{e}^{\mathrm{i}2\pi q_{xm}x} \frac{1}{\mathrm{i}2\pi} \Bigg[& \frac{1}{q_z^{(i)} - q_{zm}} \mathrm{e}^{\mathrm{i}2\pi q_{zm}z}\left(\mathrm{e}^{\mathrm{i}2\pi(q_z^{(i)} - q_{zm})z} - \mathrm{e}^{\mathrm{i}2\pi(q_z^{(i)} - q_{zm})z_1}\right) \\ & + \frac{1}{q_z^{(i)} + q_{zm}} \mathrm{e}^{-\mathrm{i}2\pi q_{zm}z}\left(\mathrm{e}^{\mathrm{i}2\pi(q_z^{(i)} + q_{zm})z_2} - \mathrm{e}^{\mathrm{i}2\pi(q_z^{(i)} + q_{zm})z}\right)\Bigg], \\ & \text{for} \quad z_1 < z < z_2. \end{aligned} \tag{20}$$

For the $m = 0$ order, this evaluates to

$$\mathrm{i}\pi \frac{q_0^2}{q_z^{(i)}} \Delta\varepsilon_r^{(0)} \mathrm{e}^{\mathrm{i}2\pi q_x^{(i)} x} \left[\mathrm{e}^{\mathrm{i}2\pi q_z^{(i)} z}(z - z_1) - \mathrm{e}^{-\mathrm{i}2\pi q_z^{(i)} z}(z_2 - z) \right]. \tag{21}$$

The contribution of the grating to the field inside the slab reads:

$$U_{1,g}(x, z) = \sum_{m=-\infty}^{\infty} \mathrm{i}\pi \frac{q_0^2}{q_{zm}} \Delta\varepsilon_r^{(m)} \mathrm{e}^{\mathrm{i}2\pi(q_{xm}x + q_{zm}z)} \frac{1}{\mathrm{i}2\pi(q_z^{(i)} - q_{zm})} \left[\mathrm{e}^{\mathrm{i}2\pi(q_z^{(i)} - q_{zm})z} - \mathrm{e}^{\mathrm{i}2\pi(q_z^{(i)} - q_{zm})z_1} \right], \quad z_2 < z < z_3 \tag{22}$$

with $q_{xm} = q_x^{(i)} + m/p$. For the $m = 0$ order, this expression evaluates to

$$\mathrm{i}\pi \frac{q_0^2}{q_z^{(i)}} \Delta\varepsilon_r^{(0)} \mathrm{e}^{\mathrm{i}2\pi(q_x^{(i)} x + q_z^{(i)} z)}(z_2 - z_1), \tag{23}$$

where $z_2 - z_1$ is the thickness of the grating layer. Note that the scattered field propagates in the $+z$ direction towards the slab layer.

From these first-order Born expressions, we see that when the slab scatters a plane wave with a certain $q_x^{(i)}$, only another plane wave with $q_x^{(i)}$ is generated. In the grating layer however, one plane wave or diffraction order can generate other diffraction orders, i.e., mixing of diffraction orders does happen there. Only if we are to calculate the second Born order, the slab layer will scatter multiple diffraction orders, as now the input field contains the diffraction orders scattered by the grating layer during the single-scattering event of the first Born order.

3.2.3 Born series convergence

The analytical expressions can give us an indication of the convergence behavior of the Born series. The expressions share a common factor $\pi\Delta\varepsilon_r q_0^2/q_z^{(i)}$ or $\pi\Delta\varepsilon_r^{(m)} q_0^2/q_{zm}$ for the field scattered by the slab or grating, respectively. The self-contribution of each layer has a complex dependence on z, e.g., Eq. (20), but if we consider Eq. (23) for instance, we see that also the thickness of the layer pops up. We could thus say that the amplitude of a diffraction order in the first Born order is approximately $\pi\Delta\varepsilon_r^{(m)} d q_0^2/q_{zm}$, with d the thickness of the structure. Compared to the unit amplitude of the incident field, this quantity indicates how fast the Born terms grow in amplitude. This expression moreover agrees with similar results for other scalar scattering problems.[8] Most importantly, the convergence thus seems to be worse for small q_{zm}, i.e., diffraction orders that make a large angle with z.

From computations of the Born series, we can also estimate the convergence rate numerically. If we have computed $N + 1$ terms (up to the Nth Born term), we compute the quantity

$$\Gamma_{\mathrm{Born}} = \left(\frac{\max_{\mathbf{r}} |U_N(\mathbf{r})|}{\max_{\mathbf{r}} |U_0(\mathbf{r})|} \right)^{1/N}, \tag{24}$$

which gives an indication at what rate each next term in the Born series grows, compared to the previous term.

4. RESULTS

As an example, we show the case of a weakly scattering grating. The considered wavelength is 633 nm. The grating material is SiO_2 ($\varepsilon_{r,\mathrm{SiO_2}} = 2.18$ at $\lambda = 633$ nm),[9] the pitch is $p = 600$ nm, and the line width is $a = p/2$. The thickness of the grating layer and the slab are 200 nm and 150 nm, respectively. Moreover, the incident field is a plane wave with $q_x^{(i)}/q_0 = 0.40$ and $q_z^{(i)}/q_0 = 0.92$.

The results of the Born-Padé method are shown in Fig. 3. The Born series diverges for this case ($\Gamma_{\mathrm{Born}} = 1.60$), but Padé approximation retrieves the electric field regardless. The approximant P_{13}^{13} is the approximant closest to the result from the finite-element method simulation in COMSOL, with an error in the modulus of the field of about 2 %.

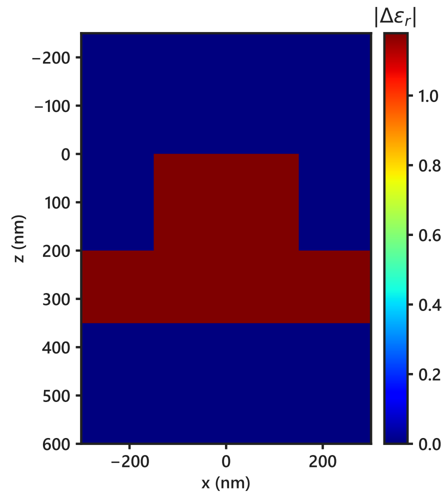

Figure 2. Grating profile of the simulated SiO_2 grating. The permittivity contrast $\Delta\varepsilon_r(x, z)$ is shown ($\varepsilon_{r,\mathrm{SiO_2}} = 2.18$).

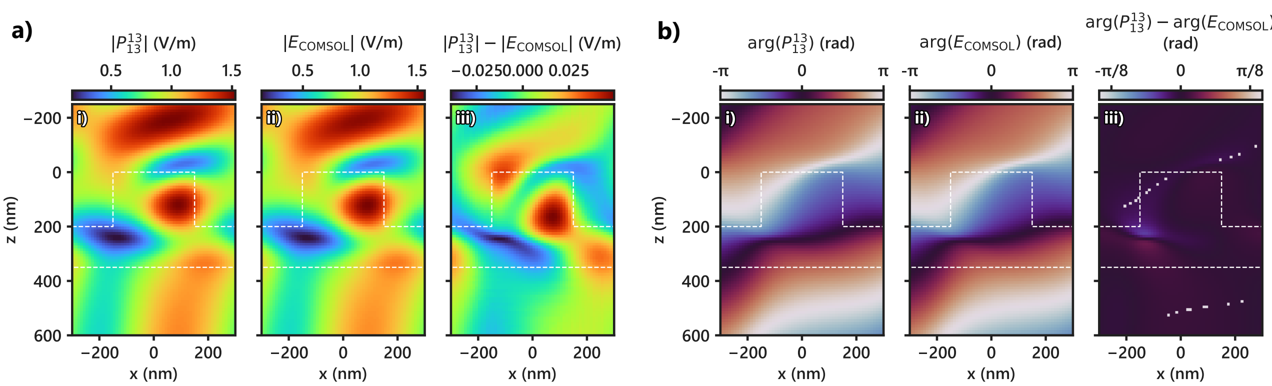

Figure 3. Electric field computed with the Born-Padé method and with COMSOL for a two-layer grating made of SiO_2 ($\varepsilon_{r,\mathrm{SiO_2}} = 2.18$): a) the modulus of the field, and b) the phase of the field. For each, the Padé approximant P_{13}^{13}, the COMSOL result, and the difference between the two is shown. The outline of the grating is shown as white dashed.

In Fig. 4, we show Γ_{Born} for various values $q_x^{(i)}$ for the example grating. Besides an increase in Γ_{Born} towards $q_x^{(i)}/q_0 = 1$ as q_z of the 0th diffraction order approaches 0, we see a peak around $q_x^{(i)}/q_0 = 0.055$. This is the $q_x^{(i)}$ for which q_z becomes 0 for the $m = -1$ diffraction order. Thus, we see worse convergence around the point where one of the diffraction orders becomes evanescent. This agrees with the behavior of the quantity discussed in Section 3.2.3, which depends on q_{zm} as $1/q_{zm}$.

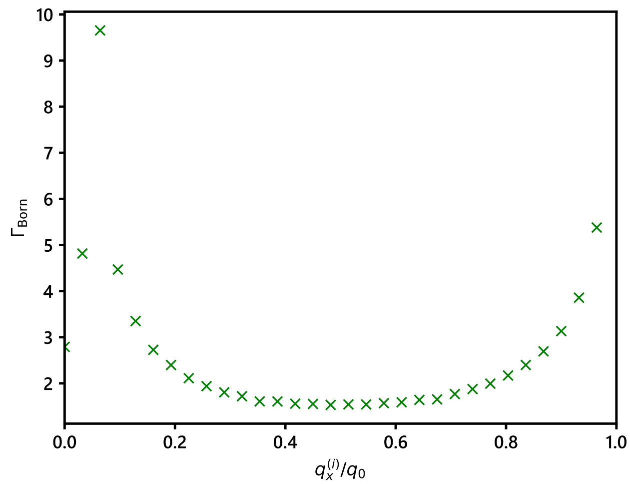

Figure 4. Convergence of the Born series for the SiO_2 grating as function of $q_x^{(i)}$ of the incident plane wave. At $q_x^{(i)}/q_0 = 0.055$, q_z for the $m = -1$ diffraction order goes to 0, explaining the peak in Γ_{Born}.

5. CONCLUSION

We have shown results for electromagnetic scattering by a 1D diffraction grating using the Born-Padé method. The Padé approximants retrieve the electric field even if the Born series diverges, and the result is accurate compared to the finite-element result in COMSOL. For the case of s polarization, analytic expressions have been derived for a simple two-layer system consisting of a grating layer on top of a slab. These expressions allow us to get an indication on the convergence rate of the Born series as function of various parameters. Most importantly, the rate is different for different diffraction orders. This is observed in the results of the Born-Padé method, as the observed convergence rate as function of $q_x^{(i)}$ increases drastically around the value for which one of the diffraction orders becomes evanescent.

APPENDIX A. VECTORIAL BORN RECURRENCE RELATION

Here, we include the vectorial equations of the Born recurrence relation for 1D diffraction gratings as derived in our previous work.[4] The input to the iteration is the induced current density $\Delta\varepsilon_r(x,z)\mathbf{E}(x,z)$, which has a Fourier series decomposition

$$\Delta\varepsilon_r(x,z)\mathbf{E}_\ell(x,z) = \sum_{m=-\infty}^{\infty} \mathbf{c}_\ell^{(m)}(z)\mathrm{e}^{\mathrm{i}2\pi(q_{xm}x + q_z^{(i)}z)}. \tag{25}$$

The Fourier coefficients $\mathbf{c}_\ell^{(m)}(z)$ are used to compute the Fourier coefficients $\mathbf{E}_{\ell+1}^{(m)}(z)$ of the next electric field Born order:

$$\begin{aligned}\mathbf{E}_{\ell+1}^{(m)}(z) = {} & \mathrm{i}\pi\frac{q_0^2}{q_{zm}}\left(\mathbf{C}_{\ell,<}^{(m)}(z)+\mathbf{C}_{\ell,>}^{(m)}(z)\right) \\ & - \mathrm{i}\pi\mathbf{q}_{\perp m}\left[\frac{1}{q_{zm}}\mathbf{q}_{\perp m}\cdot\left(\mathbf{C}_{\ell,<}^{(m)}(z)+\mathbf{C}_{\ell,>}^{(m)}(z)\right)+\hat{\mathbf{z}}\cdot\left(\mathbf{C}_{\ell,<}^{(m)}(z)-\mathbf{C}_{\ell,>}(m)(z)\right)\right] \\ & - \mathrm{i}\pi\hat{\mathbf{z}}\left[\mathbf{q}_{\perp m}\cdot\left(\mathbf{C}_{\ell,<}^{(m)}(z)-\mathbf{C}_{\ell,>}^{(m)}(z)\right)+q_{zm}\hat{\mathbf{z}}\cdot\left(\mathbf{C}_{\ell,<}^{(m)}(z)+\mathbf{C}_{\ell,>}^{(m)}(z)\right)+\frac{1}{\mathrm{i}\pi}\hat{\mathbf{z}}\cdot\mathbf{c}^{(m)}(z)\right],\end{aligned} \tag{26}$$

with

$$\mathbf{C}_{\ell,<}^{(m)}(z) = \begin{cases}\int_{z_{\min}}^{z}\mathbf{c}_\ell^{(m)}(z')\mathrm{e}^{\mathrm{i}2\pi q_{zm}(z-z')}\,\mathrm{d}z' & \text{if } z_{\min}<z, \\ 0 & \text{if } z_{\min}>z,\end{cases} \tag{27}$$

$$\mathbf{C}_{\ell,>}^{(m)}(z) = \begin{cases}\int_{z}^{z_{\max}}\mathbf{c}_\ell^{(m)}(z')\mathrm{e}^{\mathrm{i}2\pi q_{zm}(z'-z)}\,\mathrm{d}z' & \text{if } z_{\max}>z, \\ 0 & \text{if } z_{\max}<z.\end{cases} \tag{28}$$

ACKNOWLEDGMENTS

This work was funded by the Dutch Research Council (NWO), as part of the research programme Synoptic Optics (P17-24 project 3).

REFERENCES

[1] Raymond, C. J., "Scatterometry for semiconductor metrology," in [*Handbook of Silicon Semiconductor Metrology*], 389–418, CRC Press (2001).

[2] Isabella, O., Solntsev, S., Caratelli, D., and Zeman, M., "3-D optical modeling of thin-film silicon solar cells on diffraction gratings," *Progress in Photovoltaics: Research and Applications* **21**(1), 94–108 (2013).

[3] Moharam, M. G. and Gaylord, T. K., "Rigorous coupled-wave analysis of planar-grating diffraction," *Journal of the Optical Society of America* **71**, 811 (July 1981).

[4] van der Sijs, T. A., El Gawhary, O., and Urbach, H. P., "Padé approximants of the Born series of electromagnetic scattering by a diffraction grating," *Physical Review A* **109**, 033522 (Mar. 2024).

[5] van der Sijs, T. A., El Gawhary, O., and Urbach, H. P., "Padé resummation of divergent Born series and its motivation by analysis of poles," *EPJ Web of Conferences* **266**, 13035 (2022).

[6] Osnabrugge, G., Leedumrongwatthanakun, S., and Vellekoop, I. M., "A convergent Born series for solving the inhomogeneous Helmholtz equation in arbitrarily large media," *Journal of Computational Physics* (2016).

[7] Bender, C. M. and Orszag, S. A., [*Advanced Mathematical Methods for Scientists and Engineers I: Asymptotic Methods and Perturbation Theory*], vol. 1, Springer Science & Business Media (1999).

[8] van der Sijs, T. A., El Gawhary, O., and Urbach, H. P., "Electromagnetic scattering beyond the weak regime: Solving the problem of divergent Born perturbation series by Padé approximants," *Physical Review Research* **2**, 013308 (Mar. 2020).

[9] Gao, L., Lemarchand, F., and Lequime, M., "Refractive index determination of SiO2 layer in the UV/Vis/NIR range: Spectrophotometric reverse engineering on single and bi-layer designs," *Journal of the European Optical Society - Rapid publications* **8** (Jan. 2013).